Veröffentlichung

Autoren

Burnazzi, Marco;Kumar, Pradeep;Semaan, Richard;Radespiel, Rolf

Titel

NUMERICAL ASSESSMENT OF TWO PERIODIC ACTUATION APPROACHES FOR FLOW SEPARATION CONTROL

Publisher o. Konferenz

DLRK Kongress, 2014, Augsburg

Jahr

2014

Internet-Link (Doi-Nr.)

NUMERICAL ASSESSMENT OF TWO PERIODIC ACTUATION APPROACHES FOR FLOW SEPARATION CONTROL

M. Burnazzi, P. Kumar, R. Radespiel and R. Semaan
Institute of Fluid Mechanics, Technische Universität Braunschweig,
Hermann-Blenk-Straße 37, 38108 Braunschweig, Germany.

Abstract

This study investigates two actuation approaches to implement periodic tangential blowing over a gap-less high-lift flap. The high-lift configuration is composed of an active simple-hinged Coanda flap and a leading-edge droop nose device. The two approaches compared in the present work are based on different methods for obtaining a periodic oscillation of the Coanda jet. The first approach varies the jet momentum by periodically changing the slot exit section. As a result the jet velocity remains approximately constant and the mass flow drives the momentum oscillations. In the second approach, the total pressure inside the jet plenum is varied, leading to different jet velocities and mass flows. These two approaches create jets with different characteristics, which interact differently with the flow over the flap. The analysis is based on flow-field data obtained from 2D unsteady Reynolds averaged Navier-Stokes (uRANS) simulations. The two actuation approaches are compared for two different frequencies and two different amplitudes. The results show that similar flow mechanisms are obtained by the two approaches, and the resulting lift performances are comparable. However, in the case of large amplitude signals the lip-motion approach lead to smaller fluctuations of lift coefficient and to a slightly higher average lift.

1. INTRODUCTION

Improved performance of high-lift devices has been an important aerodynamic problem for decades. Several active and passive flow control techniques that aim to achieve more efficient high-lift systems can be found in the literature, such as vortex generators, Gourney flaps, synthetic jets, blowing, suction, and acoustic excitation [1-5] to name only a few. A particularly promising approach is circulation control, which has been investigated for several decades [6-8]. Circulation control with steady jets, even at very small mass flow rates, has been shown to yield lift coefficients that are comparable or superior to conventional high-lift systems [9-10]. The main issue that prevents circulation control from being widely employed in the commercial aviation industry is its large power requirements compared to the recuperated aerodynamic gains. As such, considerable effort has been undertaken in the last decades to reduce the required power through periodic actuation. Two studies during the mid-1970's investigated pulsed blowing associated with circulation control [11-12]. Results from these experiments indicated that pulsed blowing reduced the mass flow requirements for circulation control, and hence the required power. However, both experiments were limited in scope and little was revealed about the physics of the phenomena. More recently, periodic blowing on a circulation control wing with circular trailing edge was examined [13]. A 50% reduction in the required mass flow for a certain lift coefficient was achieved. It is worth noting that the periodic excitation benefits have also been demonstrated in other flow control applications, such as pulsed actuation over a flap [14-15] and acoustic excitation [16-17]. A particular variation of circulation control is tangential blowing over a highly deflected flap, which utilizes the Coanda effect to keep the flow attached. Periodic actuation of such flows requires complex mechanisms capable of varying the jet momentum over a wide range of frequencies. This issue becomes even more challenging if the fluid used for the experiments is water, which on one hand yields higher Reynolds numbers. The inertia of water, at the same time, does not allow the control of the pressure inside the plenum at the required frequencies. This problem is addressed in the present work by numerically simulating two possible actuation mechanisms. The first case simulates an oscillating piezo-electric actuator lip installed over the jet exit slot, where the area of jet exit cross-section is varied yielding a change in the jet momentum. The second case simulates the actuation of a piezo-electric valve at the plenum base that directly controls the pressure, and hence the jet velocity and the mass flow rate. These two mechanisms generate different Coanda jet characteristics, which may interact differently with the outer flow over the flap. This study analyzes the flow dynamics of the two actuation mechanisms using uRANS simulations. The efficiency of the two actuation methods, measured by lift gains, as well as the flow interaction between the jet and the outer flow are thoroughly investigated for two different frequencies and two oscillation amplitudes. The conclusions drawn by the present work represent an important element for the design of experiments involving unsteady flow actuation.

2. HIGH-LIFT CONFIGURATION

The high-lift configuration employed in the present work was designed to achieve very high lift coefficients (up to C_l=5) during take-off and landing. This high lift coefficient was only possible through the modification of the reference DLR-F15 transonic airfoil by the addition of a Coanda trailing edge flap and a droop nose leading edge device. This section briefly presents the previous work that resulted in the current design.

2.1. Trailing-edge device

The main trailing edge design parameters are the flap deflection angle, the blowing momentum coefficient, and the blowing slot height [18]. This study also showed that the flap angle and the blowing momentum coefficient should increase to achieve higher lift targets, whereas the slot height should remain small with values of around 0.0006 times the airfoil chord length. Surprisingly, the optimum slot height was found to be independent of the flap angle. The detailed curvature distribution of the Coanda surface used as flap knuckle shape was found to be less important. A radius of curvature with 0.07 times the chord length was determined to be a reasonable design choice. The flap length suited to achieve high lift gains was also identified, with the best efficiency obtained with flap lengths of 0.25-0.30 times the airfoil chord [18]. The internal shape of the duct was designed with the upper and lower walls parallel to each other at the exit section. A contraction rate of 15 was employed to obtain a realistic jet velocity profile. Figures 3 and 4 illustrate the resulting design, where the internally blown flap was set at 65° deflection angle.

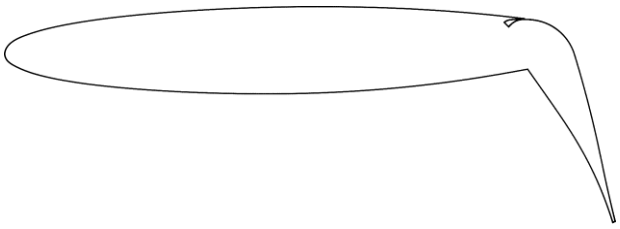

FIGURE 1. DLR F15 airfoil, equipped with an active Coanda flap

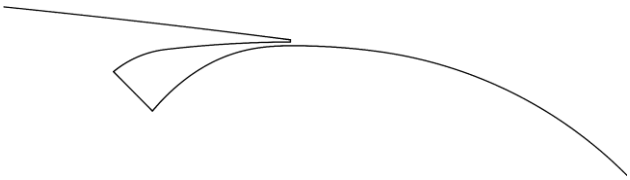

FIGURE 2. A close-up of the blowing slot

The effect of momentum coefficient is presented in Figure 3, where a reduction in the angle of attack of maximum lift with higher blowing rates is observed. As the adverse pressure gradient along the suction side grows rapidly with the angle of attack it creates significant momentum losses towards the trailing edge device. These momentum losses adversely affect the ability of the wall jet to provide flow turning. Local blowing at the nose or at other locations of the airfoil did not help much, as it extended the useful angle-of-attack range but generally at the cost of decreasing the lift gain factor [19, 20]. It is worth to note that the simulations predicted leading edge stall for the DLR F15 airfoil at lift coefficients above 6.

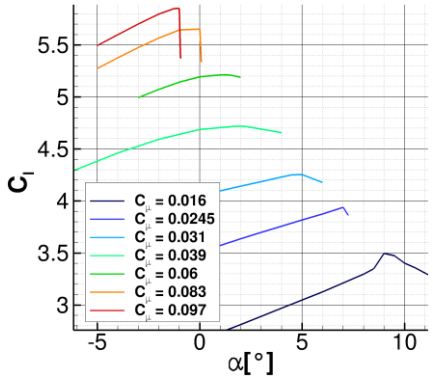

FIGURE 3. Effect of blowing momentum on the angle of maximum lift for the DLR F15 airfoil with 65° flap angle, computed for M=0.15, Re=12·10^6

2.2. Leading-edge device

The high circulation generated by the active flap dramatically reduces the stall angle of attack. This is due to the high curvature of the streamlines at the leading edge. With an increase of lift, the stagnation point moves downstream along the pressure side, accelerating the flow around the leading edge. Conventional high-lift systems employ slotted leading edge devices, slats, to address this problem. However, gaps are a major source of airframe noise during landing. Therefore, a flexible gap-less leading edge device was specially developed [21] to extend the useful angle of attack range without increasing the noise level. Details on the performances of the leading edge device, as well as a comparison with a conventional slat configuration, are discussed by Burnazzi and Radespiel [22]. This leading edge device consisted of a drooped nose, where the camber and the thickness were increased, resulting in a reduction of the suction peak at the leading edge. The morphed shape makes it possible to distribute the low pressure area over a wider surface, reducing the minimum pressure values, as shown in Figure 4, where a comparison between the clean-nose and the droop-nose configurations is presented. The load distribution of the droop nose airfoil results in a different stall behavior [22]. As a result, the stall angle of attack is increased by 13.5° yielding a lift coefficient 19.5% higher than the clean nose configuration, as reported in Table 1. Also the pitching moment coefficient is considerably improved, resulting in -11.7% at stall condition.

	$C_{l,max}$	α_{max}[°]	$C_{m,stall}$
Clean nose	5.27	1.5	-2.184
Droop nose	6.30	15.0	-2.44
Relative variation	+19.5%	+13.5	-11.7%

TAB 1. Aerodynamic comparison between the clean nose and the flexible droop nose configurations at C_μ=0.06

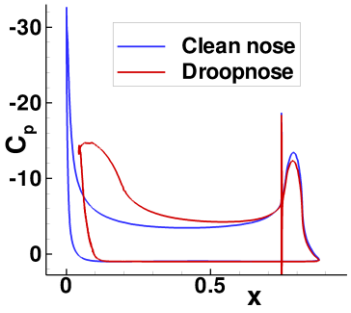

FIGURE 4. C_p distributions at stall conditions, C_μ=0.06

3. NUMERICAL APPROACH

The present investigations were based on 2D simulations of the modified DLR F15 airfoil in high-lift configuration (Figure 5). The CFD solver employed to perform the analysis was the DLR TAU-Code [23, 24], which uses a finite-volume approach for the solution of the Reynolds Averaged Navier-Stokes (RANS) equations. For the present study a central scheme for the spatial discretization of the mean flow inviscid flux, and a second order upwind Roe scheme for the convective turbulent flux were used. The turbulence model was Spalart-Allmaras with a correction due to flow rotation and curvature [25]. This last module enables the one-equation turbulence model to maintain a good accuracy in regions where the streamlines have a high curvature. This characteristic is fundamental for the simulation of the Coanda phenomenon, which is based on the equilibrium between the inertial forces and the momentum transport in the direction normal to the convex surface [26, 27]. This numerical set-up was validated by wind tunnel experiments [28]. In particular, the 3-D flow simulations that included the wind tunnel wall effects were in good agreement with the experimental results [29].

The grid employed for the present analyses contained about 250,000 points and included an unstructured region and a structured one. The structured grid layer started from the surfaces and is extended to cover the region where the main viscous phenomena occurred. It ensured y^+ lower than 1 near the wall. The grid plots of Figures 5, and 6 show some of the main features of the mesh. An important characteristic of the grid, that made it suitable for high-lift simulations, was the density of points along the pressure side, as the stagnation point were situated in this region. A large number of points was therefore necessary to properly capture the flow attachment. The structured region was extended over a large area above the flap, in order to accurately capture vortices expected in case of flow separation from the flap. The flap trailing edge was discretized by means of a local C-block topology, in order to avoid the propagation of high point density into areas where grid points were not needed and could slow the convergence down. Contrarily, a H topology was used for the trailing edge of the slot lip, as shown in Figure 6, since the grid deformation algorithm employed to adapt the grid to the lip motion could not handle a more complex grid topology.

The Coanda jet was numerically obtained by imposing the total pressure and total temperature at the base of the jet plenum. The flow established by these conditions accelerated through the converging nozzle creating the tangential wall jet. The periodic forcing was implemented in two different ways for the two actuation mechanisms. The first actuation approach was based on the variation of the jet slot exit section, which was achieved by the deformation of the lip over the slot. The lip movement was forced to maintain a smooth contour on both sides, with continuous first and second order derivatives, and to maintain the duct walls parallel at the plenum exit. These conditions were satisfied using suitable spline functions. A 3rd order polynomial function was used for the top side of the lip, whereas a 5th order one for the bottom. Figure 7 illustrates the lip deformation needed to produce the large C_μ signal amplitude used in the present analyses. For the second approach, a periodic blowing was obtained by varying the total pressure inside the jet plenum.

The results discussed in the following section were obtained for α=0.0°, M=0.15, Re=$12\cdot10^6$. The effect of the two different actuation principles was analyzed at 25Hz and 100Hz, for two amplitude levels of the forcing signal. For the dynamic-lip control, the slot height was varied by 0.5 and 2 times the nominal slot height, h=0.06% chord, with the middle position set at 0.25h. For the pressure control approach, the total pressure at the plenum boundary condition was varied in order to achieve the same C_μ distribution as obtained by the lip motion.

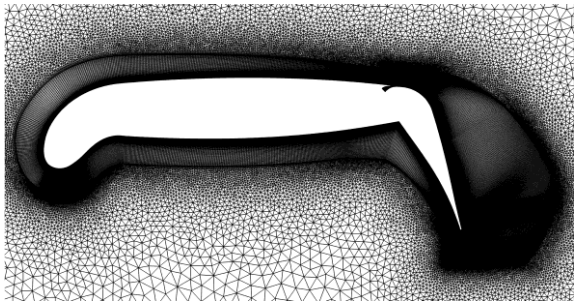

FIGURE 5. Grid around the modified DLR-F15 airfoil

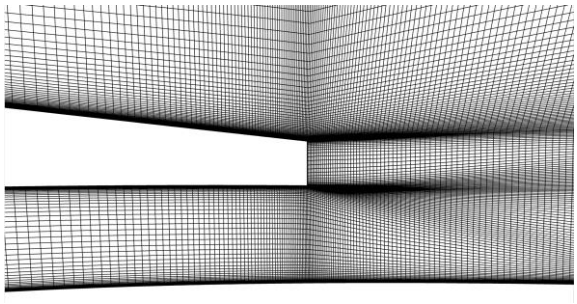

FIGURE 6. Close up of the grid at the blowing slot

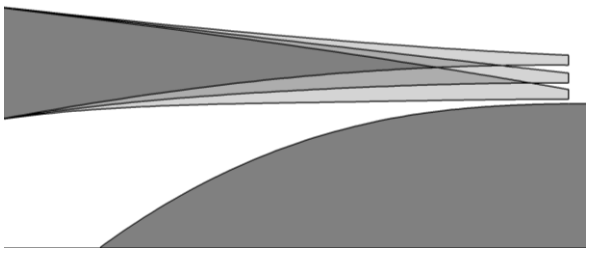

FIGURE 7. Illustration of lip deformation during a large-amplitude actuation cycle

4. RESULTS

This section discusses the results obtained by the two actuation approaches, which generated jets with the same momentum coefficients, but different velocity profiles and mass flow rates. The periodic forcing obtained by the lip motion was based on mass flow rate fluctuations caused by slot height variations, while the velocity remained essentially constant. On the other hand, varying the total pressure inside the plenum caused variations of momentum that were driven by velocity fluctuations and mass flow rate. These different jet characteristics affected the mixing dynamics between the outer flow and the jet differently. In this section, the mixing dynamics caused by the two actuation approaches are investigated by means of boundary layer velocity profiles, and the overall lift performances are described.

4.1. Mixing area

The evolution of the flow over the flap during one actuation cycle is described by means of velocity profiles extracted from 4 particular locations, illustrated in Figure 8, at 8 time instants (Figure 9). The boundary layer analysis locations were selected in order to study the interaction between the jet and the outer flow over the Coanda surface. The first location, BL1, corresponds to the jet slot exit and allows to analyze the boundary layer velocity profiles of the jet and the outer flow just before the mixing. The second location is placed at the beginning of the mixing area in order to investigate the effects of the jet characteristics on the flow mixing. Finally, the third and fourth locations show the behavior of the mixed flow in presence of the adverse pressure gradient over the Coanda surface. The corresponding results for the four tested cases are shown in Figures 10 to 13.

At the first boundary layer location, which is located at the jet exit and is referred to as BL1, both the velocity profiles of the jet and those of the outer flow are extracted. As Figures 10 to 13 show, the outer flow boundary layer velocity profiles at BL1 have similar distributions, which suggests a limited effect of the type of actuation on the outer boundary layer. The jet velocity profiles at the plenum exit illustrate the characteristics of the two momentum control approaches. With the lip-control approach the maximum jet velocity remains approximately constant throughout the actuation cycle, while the jet thickness varies. In this case, the momentum variations are driven by fluctuations of mass flow, obtained by variations of the slot height. On the other hand, the pressure-control approach generates jet velocity fluctuations, whereas the jet thickness remains constant. Therefore, the jet momentum is now controlled by both velocity and mass flow variations. At BL2, the mixing between the jet and the outer flow starts to take place. At this location, positioned at 5h from the exit section, the difference of jet velocity and thickness between the two actuations is still clearly visible. Further downstream, the mixing diffuses the jet momentum in direction normal to the flap surface, resulting in the profiles of locations 3 and 4. Here, the velocity profiles obtained by the two actuation principles appear very similar. A significant influence of the different jet characteristics is only visible with the high amplitude signals. The high amplitude signals reach a lower C_μ during the actuation cycle, which results in a large separation over the flap. During these phases, the velocity profiles extracted from BL4 show a backflow near the wall. In particular, the pressure-control actuation seems to be more sensitive to this phenomenon. For the 25Hz signal, the flow separation occurs with both actuation approaches. However, during the rising phase of the C_μ, the flow separation disappears earlier with the lip-motion approach. For the 100Hz actuation, the backflow appears only with the pressure-control approach, whereas the boundary layer obtained by the lip motion has always sufficient momentum to overcome the adverse pressure gradient in this area. During the phase of higher C_μ, the velocity profile at BL4 shows that the outer flow is significantly accelerated by the jet, and the inflection point is no longer present. The maximum velocity is reached at this location after a short delay with respect to the C_μ fluctuations, which does not show a significant difference between the two tested frequencies.

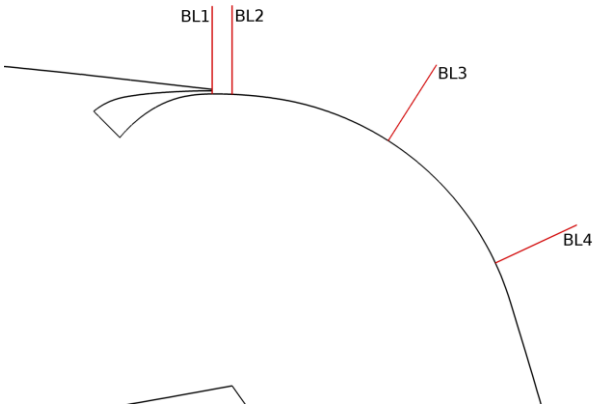

FIGURE 8. Locations of the boundary layer analysis

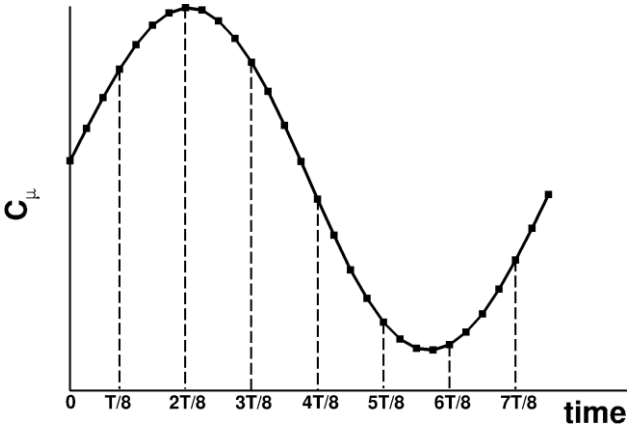

FIGURE 9. Time points through one actuation cycle

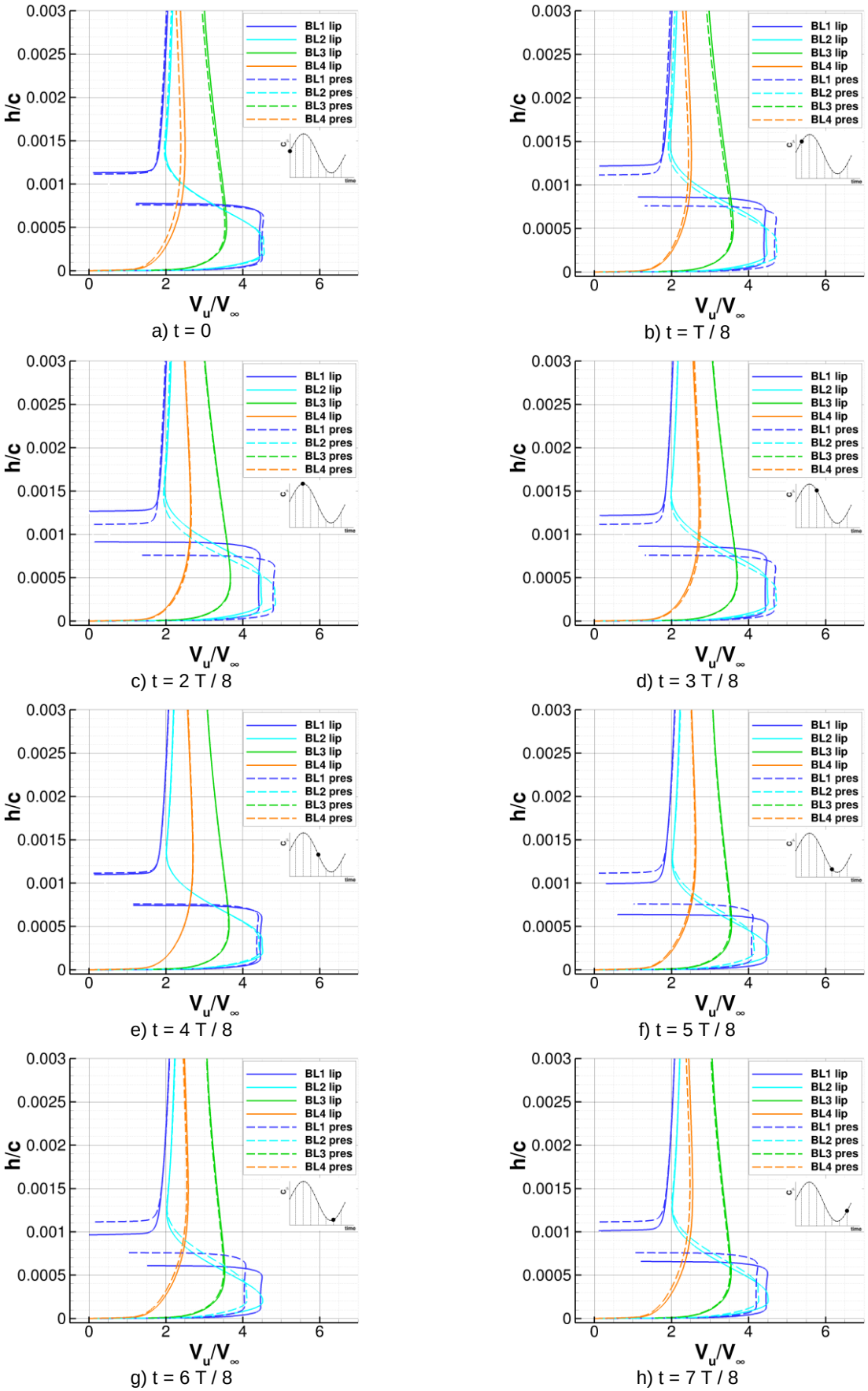

FIGURE 10. Velocity profiles at the 4 selected locations for the two actuation approaches for the 25Hz actuation frequency small amplitude case

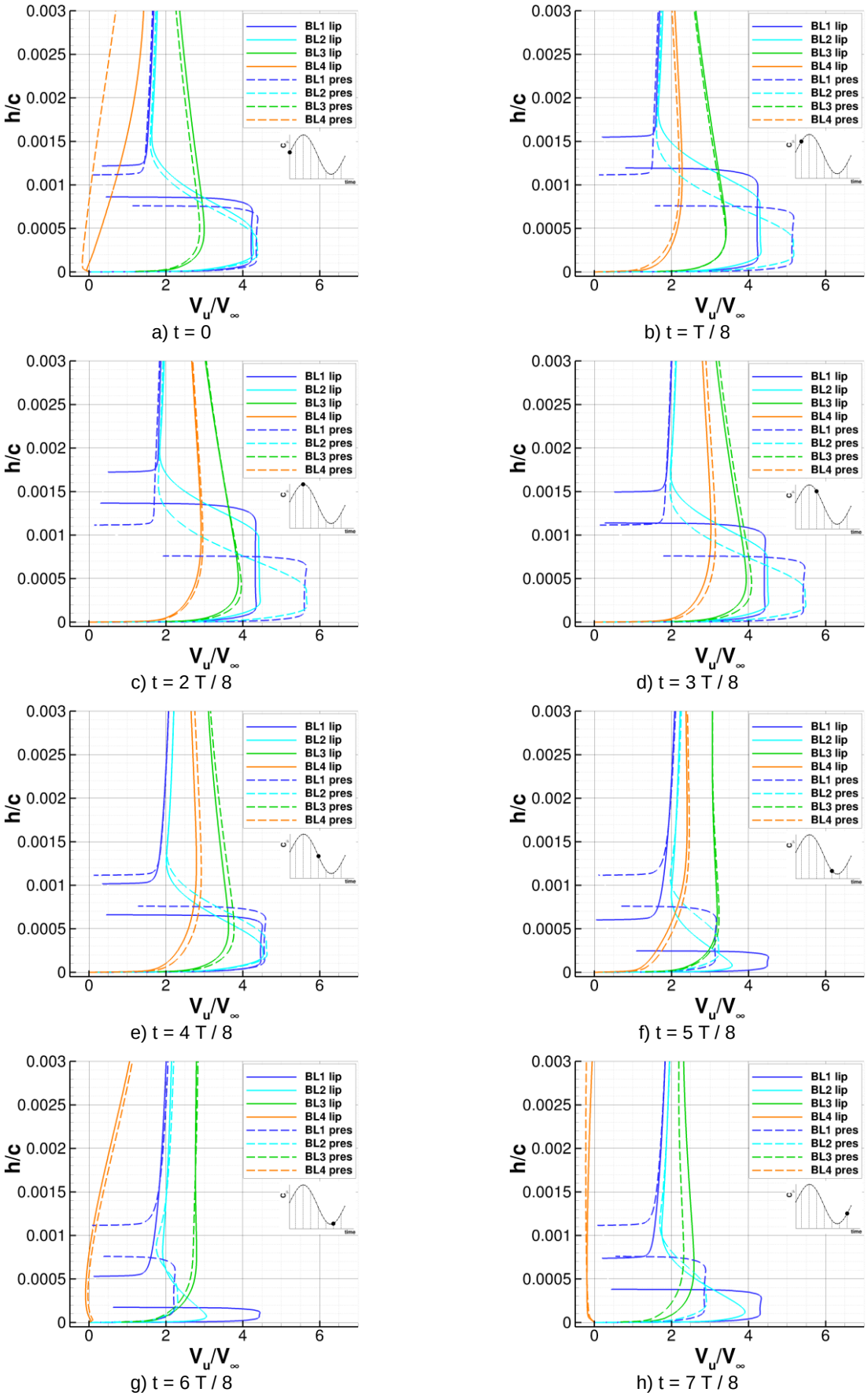

FIGURE 11. Velocity profiles at the 4 selected locations for the two actuation approaches for the 25Hz actuation frequency large amplitude case

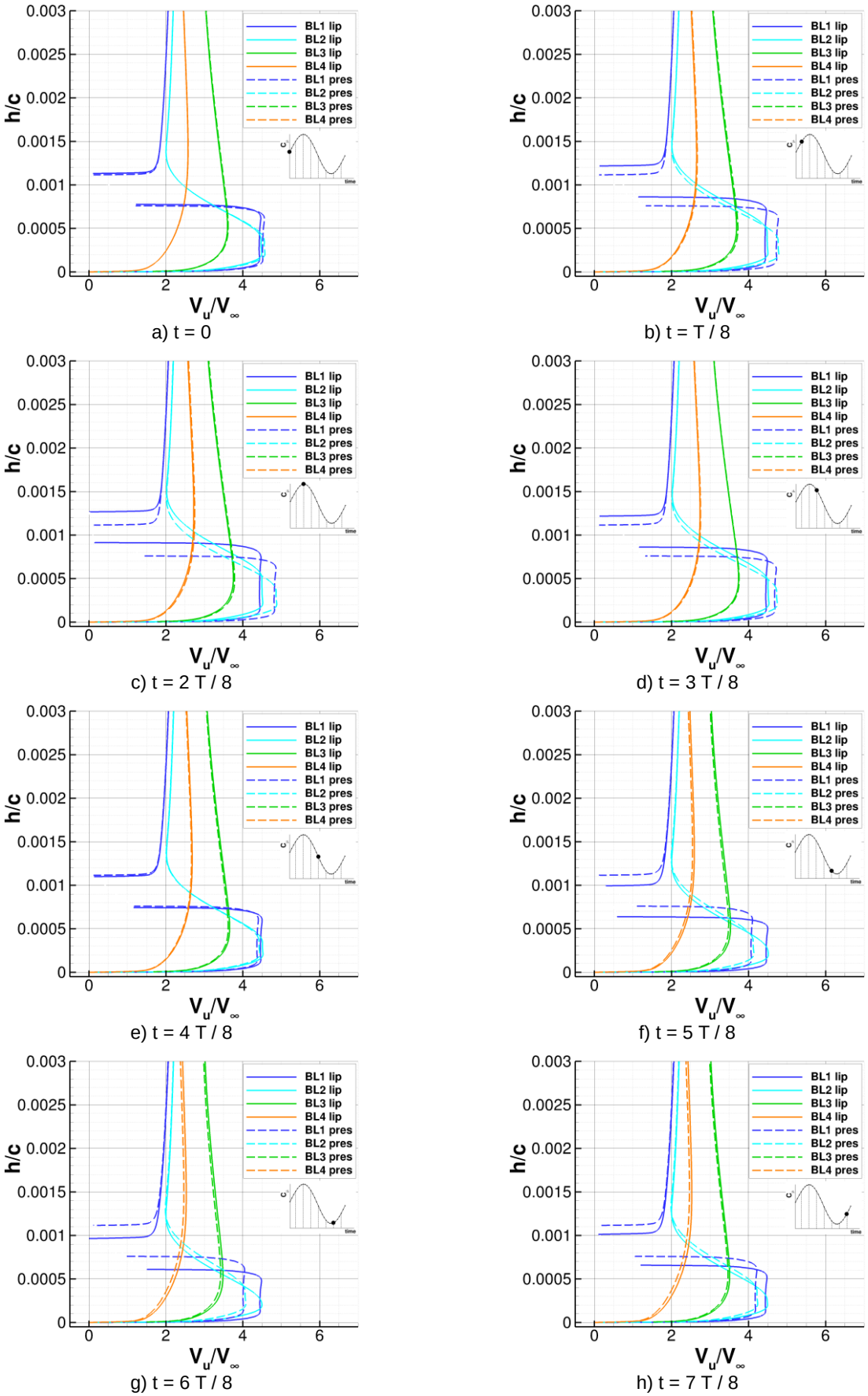

FIGURE 12. Velocity profiles at the 4 selected locations for the two actuation approaches for the 100Hz actuation frequency small amplitude case

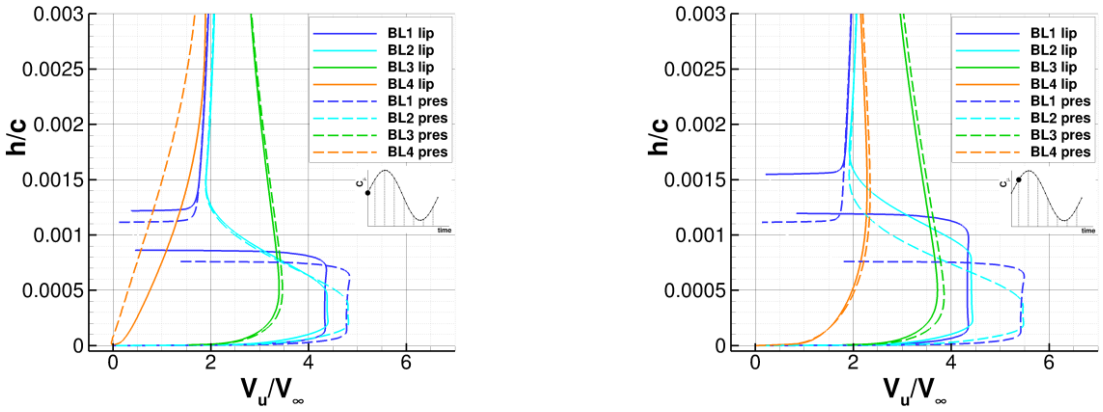

a) t = 0

b) t = T / 8

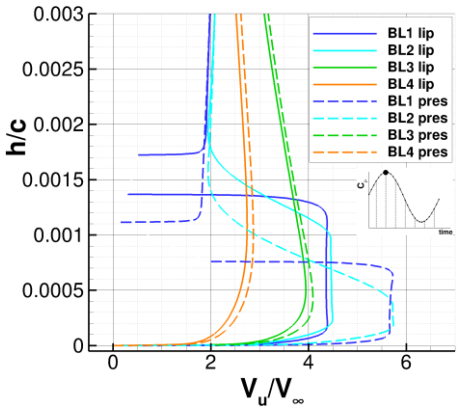

c) t = 2 T / 8

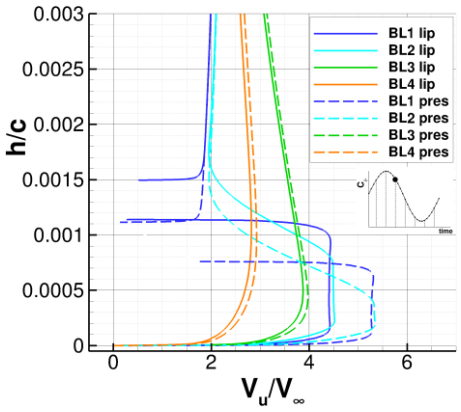

d) t = 3 T / 8

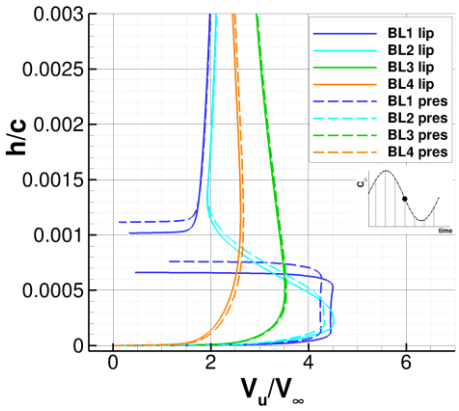

e) t = 4 T / 8

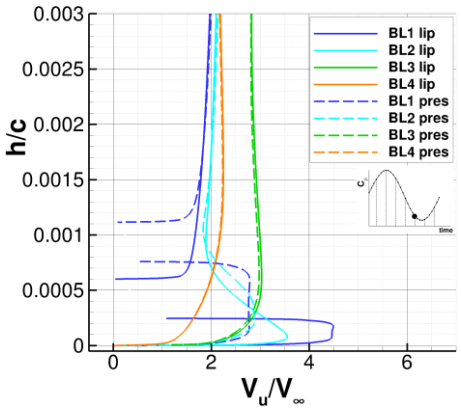

f) t = 5 T / 8

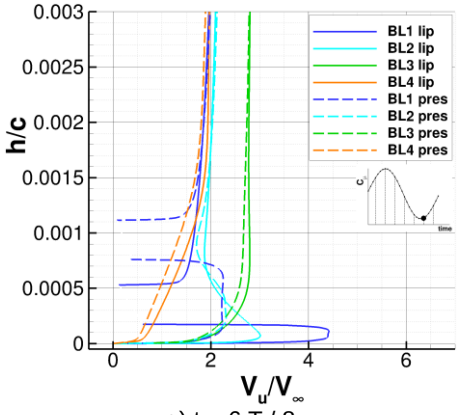

g) t = 6 T / 8

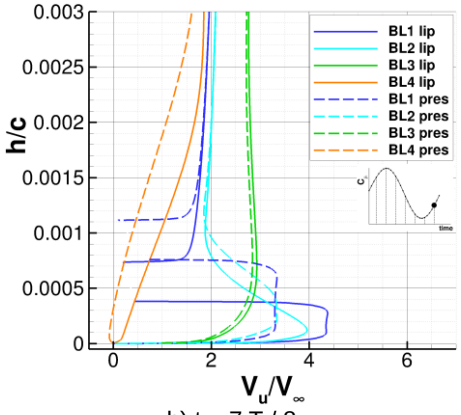

h) t = 7 T / 8

FIGURE 13. Velocity profiles at the 4 selected locations for the two actuation approaches for the 100Hz actuation frequency large amplitude case

4.2. Overall performances

In this section the lift performances resulting from the flow dynamics described above are discussed. Figure 14 and Table 2 summarize the actuation signals and the lift responses. The C_μ trends show the characteristics of the 4 test cases and describe a good agreement between the two actuation approaches. The lift coefficient follows the variation of jet momentum with a significant delay, which is dependent on the actuation frequency; ~180° for 25Hz and ~90° for 100Hz.

The C_l average values and the amplitude of the relative fluctuations are reported in Table 2. The lift response amplitude of the 100Hz cases is significantly lower than the 25Hz actuations, as shown by the standard deviations. Moreover, the 100Hz excitation yields higher average lift values. The signal amplitude seems to have an even larger effect on the lift response; the low amplitude signals lead to considerably higher lift values. The increase of the average lift with respect to the large amplitude is about 10% for the 25Hz case, and about 7.5% for the 100Hz case. The effects of frequency and amplitude on the lift performances are similar for both the lip-motion and the pressure-control approach; the average lift difference between the two approaches is less than 0.5% for all the four test cases.

The lift responses of the 25Hz cases are characterized by an irregular trend. The periodicity of the actuation signal is still present in the response, but the lift does not follow a sine trend. This is caused by the superposition of the forcing signal and the shedding frequency of the separated flow. The vortex shedding occurs downstream of the flap when the jet momentum is not sufficient to completely avoid flow separation from the flap surface. This phenomenon causes periodic fluctuations of lift, with a frequency of about 50Hz. This mechanism is superposed to the actuation signal causing a deformation of the lift response at 25Hz without significantly affecting the periodicity. On the other hand, the response to the 100Hz signal does not show significant effects of the superposition to the vortex shedding fluctuations.

	Lip motion		Pressure control	
	C_μ (SD)	C_l (SD)	C_μ (SD)	C_l (SD)
25Hz, low amplitude	0.028 (0.004)	3.649 (0.103)	0.028 (0.004)	3.644 (0.155)
25Hz, large amplitude	0.027 (0.016)	3.304 (0.367)	0.029 (0.015)	3.299 (0.405)
100Hz, low amplitude	0.029 (0.004)	3.675 (0.034)	0.028 (0.004)	3.666 (0.035)
100Hz, large amplitude	0.028 (0.016)	3.403 (0.063)	0.029 (0.016)	3.416 (0.057)

TAB 2. Average jet momentum coefficient and lift coefficient with respective standard deviations (SD).

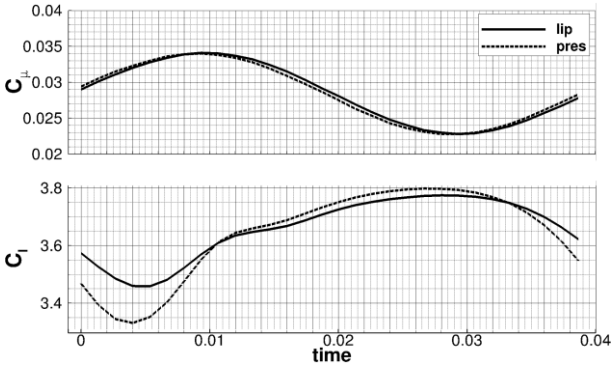

a) 25Hz low amplitude

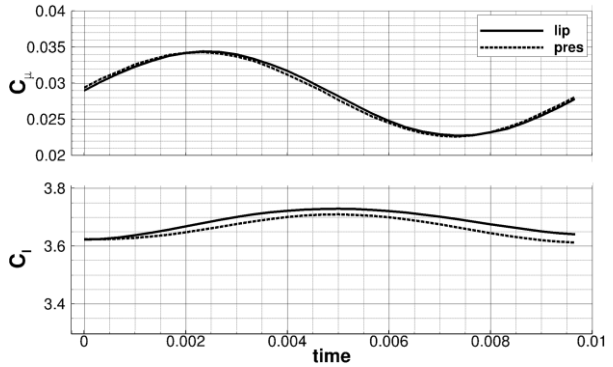

b) 100Hz low amplitude

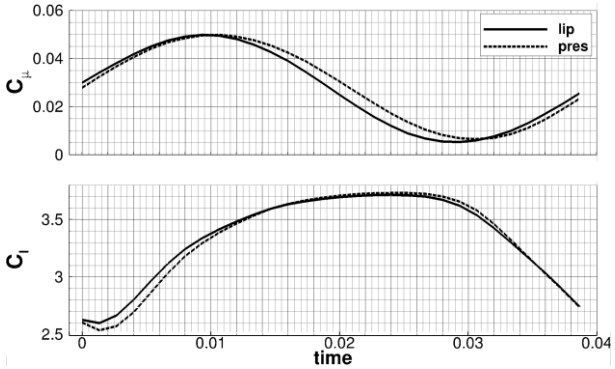

c) 25Hz large amplitude

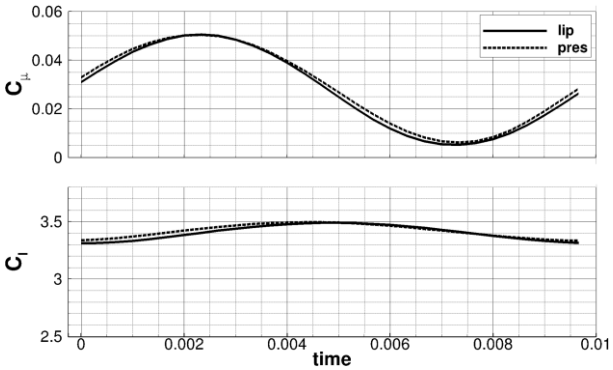

d) 100Hz large amplitude

FIGURE 14. Actuation signals and lift performances

5. CONCLUSIONS

Two practical approaches to implement periodic blowing for high-lift purposes were compared. The jet momentum fluctuations were obtained by modifying different jet characteristics, resulting in different interactions between the jet and the outer flow over the flap. One approach controlled the jet momentum by varying the mass flow and keeping the velocity constant. The other approach varied both mass flow and velocity of the jet. Two frequencies and two signal amplitudes were tested, providing a comparison basis for the two approaches.

A detailed analysis of the flow development over the Coanda surface showed that the prominent differences between the two different approaches are limited to a small region close to the blowing slot. Only under conditions of very low blowing momentum and low frequency, does the jet with constant velocity present a smaller separation, and thus a slightly larger average lift. The results also showed a similar dynamic response of the flow to the two actuation methods, which suggests that a similar underlying mechanism is behind the enhanced mixing.

The periodic control of the jet momentum is a challenge for the design of an experimental set up. The two approaches tested here are possible solutions to address this issue, presenting different practical advantages and disadvantages. The choice is typically based on the amplitude and frequency range of the required signal, as well as the fluid employed for the experiment. The present work is a new analysis of the effects of the two actuation approaches on the flow behavior and on the performances of the high-lift system, and represents a useful element for future experimental setups involving periodic circulation control.

ACKNOWLEDGEMENT

The funding of this work of the Collaborative Research Centre SFB 880 by the German Research Foundation, DFG, is thankfully acknowledged.

REFERENCES

[1] Lin J. C., Robinson S. K., McGhee R. J., and Valarezo W. O.: *Separation control on high-lift airfoils via micro-vortex generators*, Journal of Aircraft 1994; 31(6):1317–23.

[2] Storms B. L., and Jang C. S.: *Lift enhancement of an airfoil using a Gurney flap and vortex generators*, Journal of Aircraft, Vol. 31, No.3, doi:10.2514/3.46528.

[3] Jones G. S., and Englar R. J.: *Advances in Pneumatic-Controlled High-Lift Systems through Pulsed Blowing*, 21st Applied Aerodynamics Conference, AIAA 2003-3411.

[4] Karim M. A, and Acharya M.: *Suppression of dynamic-stall vortices over pitching airfoils by leading-edge suction*, AIAA J 1994 Vol 32 No 8.

[5] Ahuja K. K., and Burrin R. H.: *Control of flow separation by sound*, AIAA Journal, 84-2298, 1984

[6] Wood N., and Nielson A. J.: *Circulation Control Airfoils Past, Present, and Future*, AIAA Paper, Vols. 85-0204, 1985.

[7] Nielsen J. N., and Biggers J.: *Recent Progress in Circulation Control Aerodynamic*, AIAA Paper, Vols. 87-001, 1987.

[8] Englar R.: *Circulation control Pneumatic Aerodynamics: blown force and Moment Augmentation and Modifications; Past, Present, & Future,* AIAA Paper, Vols. 2000-2541, 2000.

[9] Sexstone M. G., Huebner L. D., Lamar J. E., McKinley R. E., Torres A. O., Burley C. L., Scott R. C., and Small W. J.: *Synergistic airframe-propulsion interactions and integrations,* National Aeronautics and Space Administration TM-1998-207644, Langely Research Center, 1998.

[10] Smith A.: *High Lift Aerodynamics, 37th Wright Brothers Lecture*, AIAA Paper , Vols. 74-939, 1974.

[11] Oyler T., and Palmer W.: *Exploratory Investigation of Pulse Blowing for Boundary Layer Control,* North American Rockwell Report NR72H-12, 1972.

[12] Walters R., Myer D., and Holt D.: *Circulation Control by Steady and Pulsed Blowing for a Cambered Elliptical Airfoil,* West Virginia University, Aerospace Engineering TR-32, 1972.

[13] Jones G. S., Viken S. A., Washburn A. E., Jenkins L. N., and Cagle C. M.: *An active flow circulation controlled flap concept for general aviation aircraft applications*, AIAA paper , Vols. 2002-3157, 2002.

[14] Petz R., and Nitsche W.: *Active separation control on the flap of a two-dimensional generic high-lift configuration,* Journal of Aircraft, vol. 3, pp. 865-874, 2007.

[15] Becker R., King R., Petz R., and Nitsche W.: *Adaptive closed-loop separation control on a high-lift configuration using extremum seeking,* AIAA journal, vol. 45, no. 6, pp. 1382-1392, 2007.

[16] Greenblatt D., and Wygnanski I. J.: *The control of flow separation by periodic excitation*, Progress in Aerospace Sciences, vol. 36, no. 7, pp. 487-545, 2000.

[17] A. Seifert, D. Greenblatt and I. J. Wygnanski, "*Active separation control: an overview of Reynolds and Mach numbers effects*," Aerospace Science and Technology, vol. 8, no. 7, pp. 569-582, 2004.

[18] Jensch, C., Pfingsten, K. C., Radespiel, R., Schuermann, M., Haupt, M., and Bauss, S.: *Design Aspects of a Gapless High-Lift System with Active Blowing*, DLRK 2009, Aachen, 2009.

[19] Jensch, C., Pfingsten, K. C., and Radespiel, R.: *Numerical Investigation of Leading Edge Blowing and Optimization of the Slot and Flap Geometry for a Circulation Control Airfoil*, Notes on Numerical Fluid Mechanics and Multidisciplinary Design, Vol. 112, Springer Verlag, 2010.

[20] Englar, R. J., Smith, M. J., Kelley, S. M., and Rover, R. C.: *Application of Circulation Control to Advanced Subsonic Transport Aircraft, Part I: Airfoil Development*, Journal of Aircraft, Vol. 31, No. 5, Sept.-Oct. 1994.

[21] Burnazzi, M., and Radespiel, R.: *Design and Analysis of a Droop Nose for Coanda Flap Applications*, AIAA Journal of Aircraft, May 2014, doi: 10.2514/1.C032434.

[22] Burnazzi, M., and Radespiel, R.: *Assessment of leading-edge devices for stall delay on an airfoil with active circulation control*, CEAS Aeronautical Journal, May 2014, doi: 10.1007/s13272-014-0112-5.

[23] Kroll, N., Rossow, C.-C., Schwamborn, D., Becker, K., and Heller, G.: *MEGAFLOW - A Numerical Flow Simulation Tool for Transport Aircraft Design*, ICAS Congress, Toronto, 2002.

[24] Schwamborn, D., Gerhold, T., and Heinrich, R.: *The DLR TAU-Code: Recent applications in Research and Industry*, ECCOMAS CFD, Egmond aan Zee, The Netherlands, 2006.

[25] Shur, M. L., Strelets, M. K., Travin, A. K., and Spalart, P. R.: *Turbulence Modeling in Rotating and Curved Channels: Assessing the Spalart-Shur Correction*, AIAA Journal, Vol. 38, pp. 784-792, 2000.

[26] Pfingsten, K. C., Jensch, C., Körber, K. V., and Radespiel, R.: *Numerical simulation of the flow around circulation control airfoils*, First CEAS European Air and Space Conference, Berlin, 2007.

[27] Swanson, R.C., and Rumsey, C.L.: *Computation of circulation control airfoil flows,* Computers and Fluids, Vol. 38, 2009, pp. 1925-1942.

[28] Pfingsten, K. C., Cecora, R. D., and Radespiel, R.: *An experimental investigation of a gapless high-lift system using circulation control*, Katnet II Conference, Bremen, 2009.

[29] Pfingsten, K. C., and Radespiel, R.: *Experimental and numerical investigation of a circulation control airfoil*, 47th AIAA Aerospace Sciences Meeting, Orlando, AIAA 2009-533.